JOURNAL OF VIROLOGY, Mar. 2003, p. 3712–3723 Vol. 77, No. 6
0022-538X/03/$08.00+0 DOI: 10.1128/JVI.77.6.3712–3723.2003

The Interaction between the Fiber Knob Domain and the Cellular Attachment Receptor Determines the Intracellular Trafficking Route of Adenoviruses

Dmitry M. Shayakhmetov,[1] Zong-Yi Li,[1] Vladimir Ternovoi,[1] Anuj Gaggar,[1,2] Helen Gharwan,[1] and André Lieber[1,2]*

Division of Medical Genetics, Department of Medicine,[1] and Department of Pathology,[2] University of Washington, Seattle, Washington 98195

Received 28 August 2002/Accepted 19 December 2002

Most of the presently used adenovirus (Ad) vectors are based on serotype 5. However, the application of these vectors is limited by the native tropism of Ad5. To address this problem, a series of fiber chimeric vectors were produced to take advantage of the different cellular receptors used by Ad of different subgroups. In this study we utilize an Ad5-based chimeric vector containing sequences encoding the Ad35 fiber knob domain instead of the Ad5 knob (Ad5/35L) to analyze factors responsible for selection of intracellular trafficking routes by Ads. By competition analysis with recombinant Ad5 and Ad35 knobs we showed that the Ad5/35L vector infected cells through a receptor different from the Ad5 receptor. Intracellular trafficking of Ad5 and Ad5/35L viruses was analyzed in HeLa cells by tracking fluorophore-conjugated Ad particles, by immunostaining for capsid hexon protein, by electron microscopy, and by Southern blotting for viral DNA. These studies showed that the interaction with the Ad35 receptor(s) predestines Ad5/35L vector to intracellular trafficking pathways different from those of Ad5. Ad5 efficiently escaped from the endosomes early after infection. In contrast, Ad5/35L remained longer in late endosomal/lysosomal compartments and used them to achieve localization to the nucleus. However, a significant portion of Ad5/35L particles appeared to be recycled back to the cell surface. This phenomenon resulted in significantly less efficient Ad5/35L-mediated gene transfer compared to that of Ad5. We also demonstrated that the selection of intracellular trafficking routes was determined by the fiber knob domain and did not depend on the length of the fiber shaft. This study contributes to a better understanding of the mechanisms that govern the infection of retargeted, capsid-modified vectors which have potential application for hematopoietic stem cell and tumor gene therapy.

At least 100 different adenoviruses (Ads) have been isolated, approximately half of which are human serotypes. Many of the human Ad serotypes have distinct pathophysiology, which has been explained by the utilization of different cell-type-specific receptors for virus attachment and entry. Recent studies also suggest that events following virus uptake, including intracellular trafficking and nuclear import, critically determine the efficacy of viral gene expression and replication. The events following viral uptake have been best studied for the Ad subgroup C serotypes 2 and 5. Ad serotypes from all subgroups A through F, except those belonging to subgroup B, are able to interact with coxsackievirus-Ad receptor (CAR) on the cell surface for the primary Ad attachment (2, 28). Subgroup C Ads then rapidly enter cells by endocytosis facilitated by interaction of the Ad penton base protein with vitronectin-binding integrins on the cell surface, including $\alpha_v\beta_3$, $\alpha_v\beta_5$, $\alpha_M\beta_2$, and $\alpha_5\beta_1$ integrins (1, 28, 32). Endosomal membranes are subsequently lysed by Ad, allowing the escape of capsids to the cytosol (3, 10, 11). Then Ad5/Ad2 particles migrate to the nucleus by using the cellular microtubule network, bind to the nuclear pore complexes, and translocate the viral genomes into the nucleus (9, 12, 26).

* Corresponding author. Mailing address: Division of Medical Genetics, Department of Medicine, Box 357720, University of Washington, Seattle, WA 98195. Phone: (206) 221-3973. Fax: (206) 685-8675. E-mail: lieber00@u.washington.edu.

For Ad5, CAR functions only as a dock for the capsid to bring itself into proximity with integrins, and CAR-mediated signaling is not required for virus internalization and trafficking. This is supported by the observation that infection of Ad5 also occurs in the absence of the cytosolic and membrane-spanning CAR domains (31). However, the interaction with and activation of integrins is critical for virus internalization. Besides facilitating virus internalization, most probably via clathrin-coated pits (29, 30), $\alpha_v\beta_3$ and $\alpha_v\beta_5$ integrins contribute to Ad-dependent permeabilization of the plasma membrane (32), activation of small G proteins of the Rho family, activation of phosphatidylinositol 3-OH kinase, Raf and extracellular receptor kinase 1 and 2 pathways (16), and protein kinase C (17). Activation of these downstream effectors of integrins results in efficient Ad internalization, escape of partially disassembled capsids from the endosome, and ultimately nuclear targeting of the Ad genome (16).

Ad5-based vectors have found widespread application as gene transfer vehicles. However, utilization of these vectors in vivo has been limited by the native tropism of Ad5. To expand the host range of Ad5 vectors, a series of fiber-chimeric vectors have been produced to take advantage of the difference in viral receptors between subgroups (14, 24, 33). For example, chimeric Ad vectors expressing an Ad3 knob/Ad5 shaft fiber protein exhibited increased transduction of human fibroblasts, monocytes, B-lymphoid cell lines, and squamous carcinoma cell lines compared to that of Ad5 vectors (24). Our group

developed a capsid-modified Ad vector containing sequences encoding the Ad35 fiber knob instead of the corresponding Ad5 knob domain (21). The chimeric Ad5/35L vector interacts with a cellular receptor(s) different from CAR and infects human hematopoietic cells and CAR^{low} breast cancer cell lines, both of which are relatively refractory to infection with standard Ad5-based vectors (20, 22). Recently, a number of investigators also began to construct new Ad vectors based on subgroup B viruses (Ad35 and Ad11) (19, 27).

Considering these new directions in the development of Ad vectors, a better understanding of factors that govern the transduction efficiency or pathways of modified Ad vectors is important. Miyazawa et al. recently demonstrated that the intracellular trafficking of the subgroup B Ad (Ad7) differs from that of subgroup C (Ad5); Ad5 rapidly escaped from early endosomes while Ad7 accumulated in late endosomes. The authors concluded that the differences in the intracellular trafficking of Ad5 and Ad7 are due to specific structures within the fiber that are involved in triggering pH-dependent membrane lysis and escape to the cytosol (13, 14). In this study, we have analyzed the intracellular trafficking of Ad5/35L in comparison to that of Ad5. We found that the selection of intracellular trafficking routes is determined by the fiber knob domain and by the nature of the primary attachment receptor. The intracellular trafficking route, in turn, determines the efficiency of gene transfer.

MATERIALS AND METHODS

Cells and viruses. HeLa (human cervix carcinoma, ATCC CCL-2.2) and 293 cells (Microbix, Toronto, Canada) were maintained in a solution containing Dulbecco's modified Eagle medium (DMEM), 10% fetal calf serum, 2 mM L-glutamine, and Pen/Strep. The following Ad vectors, which were previously constructed and described in detail, expressing green fluorescent protein (GFP) or β-galactosidase as reporter genes were used: Ad5L, Ad5S, Ad5/35L, and Ad5/35S (21). For amplification, all Ads were amplified in 293 cells under conditions that prevented cross-contamination. Viruses were banded in CsCl gradients, dialyzed, and stored in aliquots as described elsewhere (4). Ad genome titers were determined by quantitative Southern blotting. Virion DNA extracted from the purified virus particles for each particular Ad vector was run on agarose gels in serial (twofold) dilutions. A standard DNA of known concentration (purified Ad5 DNA, the concentration of which was determined by measuring optical density at 260 nm [OD_{260}]) was also applied on the same gel in serial dilutions. After transfer onto Hybond N+ nylon membrane (Amersham, Piscataway, N.J.), filters were hybridized with a labeled DNA probe (8-kb *Hin*dIII fragment, corresponding to the E2 region of the Ad genome) and DNA concentrations were measured by PhosphorImager for each particular viral preparation. These values were used to calculate a genome titer for each virus stock used. For each Ad vector used in this study at least two independently prepared virus stocks were obtained and characterized by PFU titering on 293 cells and genome titering by Southern blot.

Labeling of Ads with [^{3}H]-*methyl* thymidine and Cy3 fluorochrome. Ad5-GFP and Ad5/35L-GFP vectors were labeled with [^{3}H]-*methyl* thymidine (Amersham, Arlington Heights, Ill.)as described in detail elsewhere (22). Briefly, 5×10^7 293 cells were grown in 175-cm^2 flasks with 15 ml of DMEM–10% fetal calf serum and infected with Ad vectors at a multiplicity of infection (MOI) of 50 or higher. Twelve hours postinfection, 1 mCi of [^{3}H]-*methyl* thymidine was added to the media and cells were further incubated at 37°C until complete cytopathic effect was observed. Cells were then harvested, pelleted, washed once with cold phosphate-buffered saline (PBS), and resuspended in 5 ml of PBS. Virus was released from the cells by four freeze-thaw cycles. Cell debris was removed by centrifugation, and viral material was subjected to ultracentrifugation in CsCl gradients and subsequent dialysis as previously described (4). Virus purification and dialysis removed unincorporated radioactivity. Ad particle concentrations were determined spectrophotometrically by measuring the OD_{260}, utilizing the extinction coefficient for wild-type Ad5 of $\varepsilon_{260} = 9.09 \times 10^{-13}$ OD ml cm $virion^{-1}$. The virion-specific radioactivity was measured by a liquid scintillation counter and was always in the range of 10^{-5} to 10^{-4} cpm per virion.

To label Ad capsids with Cy3 fluorochrome (Cy3 Bifunctional Reactive Dye, PA23000; Amersham Pharmacia Biotech, Buckinghamshire, United Kingdom), we used the manufacturer's protocol without any modifications. The ratio between the volumes of Ad and labeling reagent was 1/9. After a 30-min labeling reaction, viruses were dialyzed against a solution containing 10 mM Tris-HCl (pH 7.5), 10 mM $MgCl_2$, and 10% glycerol at 4°C to remove unincorporated chemicals. The concentrations of Cy3-labeled viruses were then determined by quantitative Southern blotting as described above.

Attachment and internalization assays. These studies were performed based on a protocol published elsewhere (22). For attachment studies, 3.5×10^5 cells were incubated for 1 h on ice with equal amounts of [^{3}H]-thymidine-labeled Ad particles at an MOI of 8,000 genomes per cell in 100 μl of ice-cold adhesion buffer (DMEM supplemented with 2 mM $MgCl_2$, 1% bovine serum albumin, and 20 mM HEPES). Next the cells were pelleted by centrifugation for 4 min at $1,000 \times g$ and washed two times with 0.5 ml of ice-cold PBS. After the last wash the cells were pelleted at $1,500 \times g$, the supernatant was removed, and the cell-associated radioactivity was determined by a scintillation counter. The number of viral particles bound per cell was calculated by using the virion-specific radioactivity and the number of cells. To determine the fraction of internalized [^{3}H]-thymidine-labeled adenoviral particles, cells were incubated on ice for 1 h with the corresponding virus, washed with PBS as described above, resuspended in 100 μl of adhesion buffer, and then incubated at 37°C for 30 min. Following this incubation cells were diluted threefold with cold 0.05% trypsin–0.5 mM EDTA solution and incubated at 37°C for an additional 5 to 10 min. This treatment removed 99% of attached radioactivity. Finally, the cells were pelleted at $1,500 \times g$ for 5 min, the supernatant was removed, and the protease-resistant counts per minute were measured. Nonspecific binding of Ad particles to cells on ice was determined in the presence of a 100-fold excess of unlabeled virus. This value routinely represented less than 0.1% of viral load.

Ad infection of cells and competition assay. HeLa cells (2.5×10^5) were seeded on each well of 12-well plates 1 day before infection. One day later the actual number of attached cells per well was determined and virus was added at the indicated MOIs (number of viral genomes per cell) in 400 μl of growth medium. Cells were incubated for 6 h at 37°C. Virus-containing media was then removed and cells were washed once with PBS and then incubated in normal medium for 24 h before analysis by flow cytometry. In infection competition experiments, recombinant purified knob domains of Ad5 (35) or Ad35 were applied to cells at a concentration of 100 μg/ml 30 min before virus infection. Virus-containing media were then added to cells, incubated, and analyzed as described above. For production of recombinant Ad35 knob, a PCR fragment containing the Ad35 knob domain sequence was cloned into pQE30 (Qiagen, Valencia, Calif.) and recombinant Ad35 knob protein was then expressed in *Escherichia coli* and purified as described elsewhere for Ad5 (35).

Analyses of Ad trafficking. HeLa cells (5×10^4 cells per well) were plated onto 8-chamber glass slides in normal growth medium 1 day before infection. Twenty four hours later cells were washed with cold PBS, and Cy-3 labeled Ads were added to cells for pulse infection in a total volume of 100 μl of medium with different amounts of virus, from 1×10^9 to 4×10^{10} virus particles per ml. After incubation at 37°C for 15 min, virus-containing medium was removed and cells were incubated in growth medium for the indicated periods of times before fixation in a methanol-acetone mixture (1:1 [vol/vol]). For analysis of Ad attachment, cells were incubated with viruses for 15 min at 37°C, washed with cold PBS, and immediately fixed for further analyses. For analyses of Ad particle localization within the cells, fixed cells were incubated with primary polyclonal rabbit anti-Cathepsin B antibody Ab-3 (Oncogene, Boston, Mass.) (1/40 dilution) for 1 h at 37°C. The binding of primary antibody was developed with a 1/200 dilution of Alexaflour-488-conjugated goat anti-rabbit secondary antibody (Molecular Probes, Eugene, Oreg.) at room temperature for 30 min and was visualized on a Leica fluorescent microscope. For confocal microscopy analyses cells were infected with unlabeled Ad vectors as described above, fixed with acetone, and stained for Ad hexon protein by using fluorescein isothiocyanate-conjugated goat polyclonal anti-Ad5 hexon antibody (1/50) (Chemicon, Temecula, Calif.) for 1 h at 37°C. Acquisition of cell images was done by using a Leica confocal microscope. To analyze Ad trafficking in the presence of nocodazole, HeLa cells were preincubated with drug (20 μM) for 1 h before infection and virus- and nocodazole-containing medium was added until cells were fixed and analyzed as described above.

EM studies. For electron microscopy (EM) analyses of virus distribution, HeLa cells were infected with Ad vectors at an MOI of 1,000 genomes per cell. At the indicated time points cells were fixed with 2% glutaraldehyde in PBS with subsequent fixation in 1% OsO_4–phosphate buffer. Cells were then embedded in

Medcast (Ted Pella, Redding, Calif.), and ultrathin sections were stained with uranyl acetate and lead citrate. Processed grids were evaluated and photomicrographed with a Phillips 410 electron microscope operated at 80 kV (magnification, ×21,000). For each particular Ad vector the intracellular distribution was analyzed by counting at least 100 virus-containing cells.

Southern blot. Extraction of genomic DNA, labeling of DNA fragments, and hybridization were performed as described earlier (4).

RESULTS

Ad5 and Ad5/35L vectors interact with different attachment receptors on HeLa cells. To analyze the role of the primary attachment receptor in selection of intracellular trafficking routes by Ad vectors, we utilized two previously constructed Ad viruses, Ad5-GFP and Ad5/35L-GFP, containing identical GFP expression cassettes (21). Ad5-GFP has an unmodified wild-type Ad5 capsid, whereas the Ad5/35L-GFP vector possesses modified fibers with the knob domain derived from human serotype Ad35 (subgroup B). Ad35 has been shown to interact with a primary attachment receptor(s) different from the Ad5 receptor, CAR, on K562 human erythroleukemia cells (22). The binding rate constant of Ad5/35L-GFP virus to its receptor on 293 cells was comparable to that of Ad5-GFP (1.2×10^{10} M^{-1} and 1.44×10^{10} M^{-1}, respectively) (21).

Attachment and internalization of Ad5-GFP and Ad5/35L-GFP were analyzed after incubation of HeLa cells with [^{3}H]-thymidine-labeled viruses. HeLa cells were selected because they are susceptible to both Ad5 and Ad5/35 infection (21). Furthermore, there is a substantial amount of data accumulated on the intracellular trafficking of wild-type subgroup C and B Ads in HeLa cells (5, 7, 18). Ad5/35L-GFP vector attached to and internalized into HeLa cells approximately three times more efficiently (1,500 virus particles per cell) than Ad5-GFP vector (550 virus particles per cell) (Fig. 1A). These data were further corroborated by quantitative Southern blotting for viral genomes from particles attached to or internalized by HeLa cells (Fig. 1B). When the cells were exposed to equal amounts of virus (see Load lanes), at least three times more Ad5/35L-GFP vector genomic DNA was associated with cells than that of Ad5-GFP DNA (Ad5/35L-GFP versus Ad5-GFP Attachment and Internalization lanes). To confirm that a subgroup C fiber knob-containing virus (Ad5-GFP) and a subgroup B fiber knob-containing virus (Ad5/35L-GFP) infect HeLa cells via interaction with different attachment receptors, transduction studies were performed in the presence of the recombinant purified Ad5 or Ad35 knob domains as competitors (Fig. 1C). At all MOIs applied, the purified Ad5 knob domain was unable to block Ad5/35L-GFP infection and, correspondingly, the purified Ad35 knob domain was unable to decrease the efficiency of Ad5-GFP infection. On the other hand, Ad5 knob efficiently blocked Ad5-GFP infection of HeLa cells even at high MOIs (400 virus particles per cell). Similarly, the Ad35 knob domain efficiently blocked Ad5/35L-GFP infection. Taken together, one can conclude that Ad5-GFP and Ad5/35L-GFP vectors have identical capsids except for the fiber knob domains, which interact with two distinct primary attachment receptors.

Interaction between the fiber knob and the primary attachment receptor determines the intracellular trafficking route of Ad vectors. To analyze the intracellular trafficking of Ad5-GFP and Ad5/35L-GFP vectors, their capsids were chemically labeled with Cy3 fluorophore (11). Miyazawa et al. have previously demonstrated that the analyses of intracellular virus distribution by in situ hybridization for Ad DNA and tracing the Cy3-labeled Ad particles by fluorescent microscopy gave comparable results (14). In our study, HeLa cells were analyzed 15 min after infection to assess virus uptake and at 2 h postinfection, a time point for which most Ad5-GFP particles have been found in the perinuclear space in previous studies (11, 13). Fifteen minutes after virus uptake was initiated by transferring cells incubated with virus from ice to 37°C, the distribution of Cy3-labeled Ad5-GFP and Ad5/35L-GFP virus particles was comparable, indicating similar uptake kinetics (Fig. 2A and B, 15-min panels). In agreement with the studies shown in Fig. 1, more Ad5/35L-GFP virus particles than Ad5-GFP particles attached to HeLa cells after incubation of cells with equal virus concentrations. However, the distribution of Ad5 and Ad5/35L virions differed at 2 h postinitiation. The majority of Ad5-GFP virus particles were localized to the perinuclear space (Fig. 2, 120 min). In contrast, Ad5/35L-GFP virus particles were widely distributed throughout the cytoplasm, with high local concentrations in areas presumably involved in cell adhesion. Immunofluorescence analysis for capsid hexon protein as an alternative method for detection of viral particles yielded the same intracellular distribution patterns as seen with Cy3-labeled viruses, indicating that the covalent linking of the capsid proteins with Cy3 did not destroy capsid structures involved in intracellular trafficking (Fig. 2B).

To investigate the association of viral particles with specific cytoplasmic compartments, we infected HeLa cells with Cy3-labeled Ad5-GFP or Ad5/35L-GFP in the presence of Dextran-488, a marker for early endosomes and transporting/sorting endosomes (11). This study failed to reveal any significant colocalization of virus particles with early-intermediate endosomal compartments (data not shown). Furthermore, cells infected with Cy3-Ads (red) were subjected to immunofluorescence analyses with an antibody directed against Cathepsin B (green) (Fig. 3A). Cathepsin B is considered to be a marker for late endosomes/lysosomes (6). Ad5-GFP virus particles did not colocalize with Cathepsin B-containing compartments at 15 and 120 min postinfection. In contrast, Ad5/35L-GFP virus considerably overlapped (yellow) with Cathepsin B-positive staining, starting 15 min postinfection. This colocalization became more prominent by 2 h postinfection, when the majority of Ad5/35L-GFP virus particle were residing within the late endosomal/lysosomal compartments. Local accumulations of Ad5/35L-GFP virus particles at the cell periphery and at adhesion foci also stained positive for anti-Cathepsin B. Interestingly, the size and intensity of these signals increased over time, suggesting a potential retrograde transport of viral particles to the cell periphery within Cathepsin B-containing compartments. Plus-end trafficking of endosomes (away from the microtubuli organizing center, located in proximity to the nucleus) depends on an intact cytoplasmic microtubule network (26). To test whether this retrograde trafficking of Ad5-GFP and Ad5/35L-GFP particles involves microtubuli, we infected HeLa cells with Ad vectors after preincubating them with nocodazole, an agent that depolymerizes the microtubule network (12). In agreement with data published earlier (12), nocodazole treatment did not inhibit minus-end-directed trafficking of Ad5-GFP vector. However, nocodazole prevented

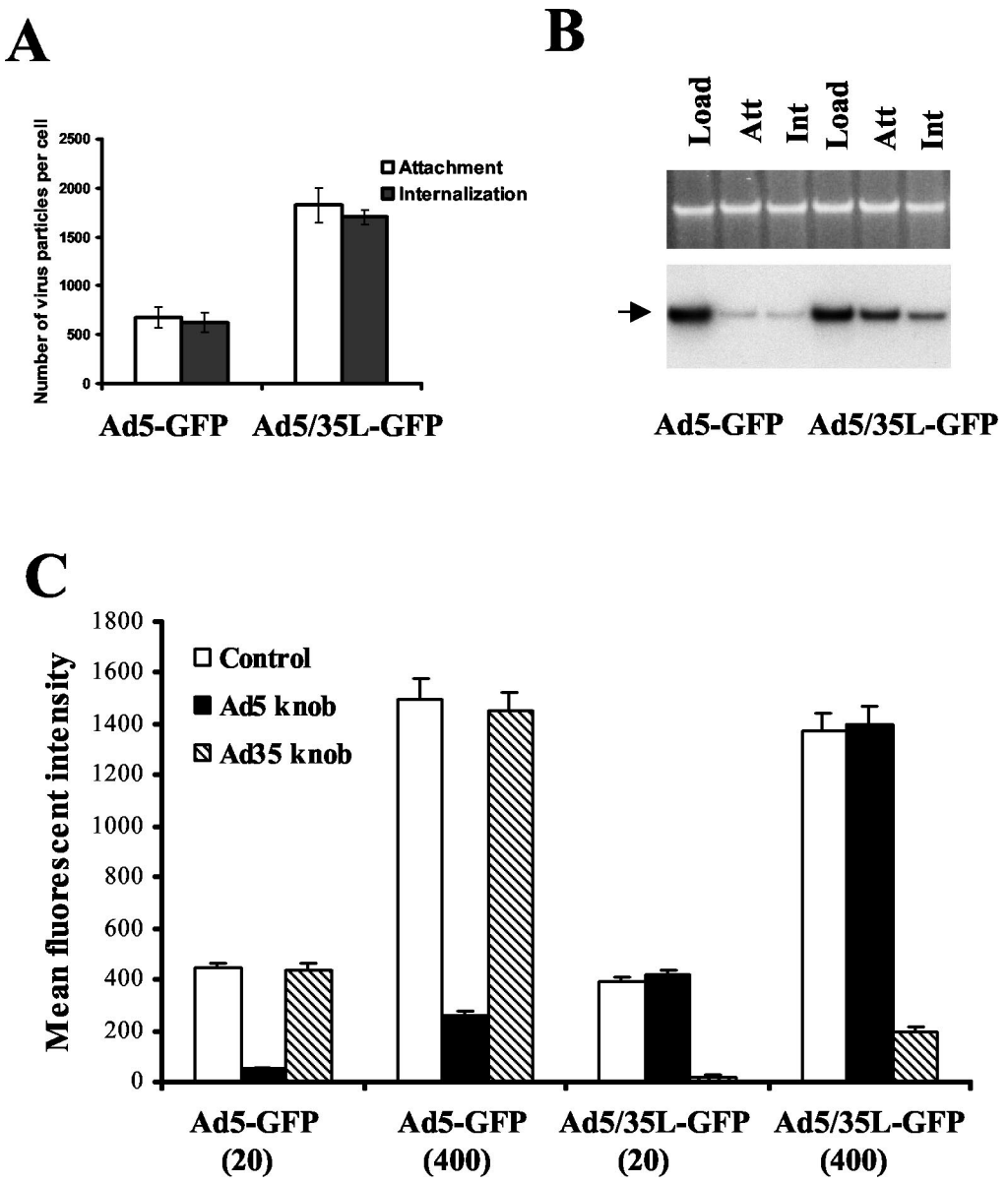

FIG. 1. Interaction of Ad5-GFP and Ad5/35L-GFP vectors with HeLa cells. (A) Attachment and internalization of [^{3}H]-thymidine-labeled Ad5-GFP and Ad5/35L-GFP vectors into HeLa cells. (B) Southern blot analysis of Ad genomes after attachment (Att) and internalization (Int) into HeLa cells. (C) Infection of HeLa cells with Ad vectors in the presence of different fiber knob domains. HeLa cells (2.5×10^5 per well of a 12-well plate) were infected in triplicates with Ad5-GFP or Ad5/35LGFP vectors at indicated MOIs (virus particles per cell) in the absence (Control) or in the presence of a 100-μg/ml concentration of purified Ad5 or Ad35 knob domain. Twenty four hours later the efficiency of gene transfer was analyzed by flow cytometry.

the accumulation of Ad5/35L-GFP virus at the cell adhesion foci and the cell periphery. Instead, the majority of virus particles was visible in the perinuclear space (Fig. 3B). This suggests that plus-end-directed (retrograde) Ad5/35L-GFP trafficking depends on the nocodazole-sensitive microtubule network.

To confirm the immunohistology data, the intracellular distribution of viral particles was further analyzed by EM (Fig. 4). HeLa cells were infected with Ad5-GFP or Ad5/35L-GFP vectors at an MOI of 1,000 virus particles per cell, and 2 h later cells were fixed and processed for EM analysis. The intracellular distribution of virus particles was assessed for at least 500 virus particles per variant (Table 1). For Ad5-GFP, 52.4% of virions were found free in the cytoplasm, 35.1% were localized to the perinuclear space (with a distance between the nuclear envelope and virus particles corresponding to less than 3 virions) (16), and only 3% of Ad5-GFP virus particles were associated with endosome-like structures. In contrast, 62.6% of Ad5/35L-GFP virus particles were colocalized with endosomal compartments, and only 13.3% of virions were found free in the cytoplasm. Importantly, many of these virions appeared to be associated with membrane structures.

To further corroborate that Ad5/35L particles utilize late endosomes/lysosomes for trafficking to the nucleus, we per-

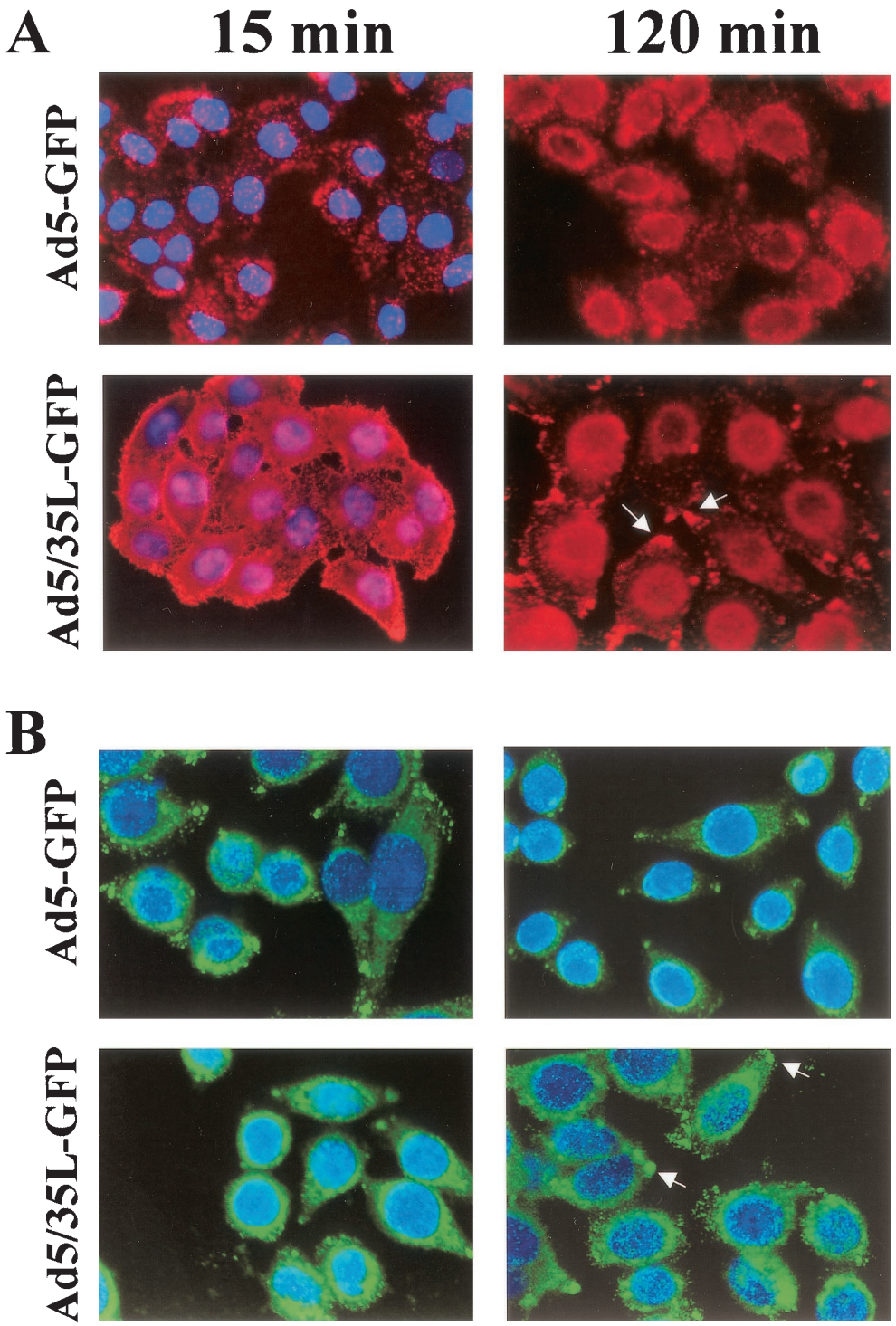

FIG. 2. Intracellular trafficking of Ad vectors in HeLa cells. (A) Migration of Cy3-labeled Ad particles to the perinuclear space at 15 min and 2 h postinitiation of virus internalization detected by fluorescent microscopy. (B) Intracellular distribution of unlabeled Ad vectors in HeLa cells 15 min and 2 h postinitiation of infection detected by immunostaining of infected cells with anti-hexon antibody and analyzed by confocal fluorescence microscopy. Primary staining with anti-hexon antibody was developed with secondary Alexa-488-conjugated antibody (green), and cell nuclei were contra-stained with 4′,6′-diamidino-2-phenylindole (blue). The accumulations of Ad5/35L-GFP virus particles at the cell adhesion foci are indicated by the arrows. The representative fields are shown at a magnification of ×200.

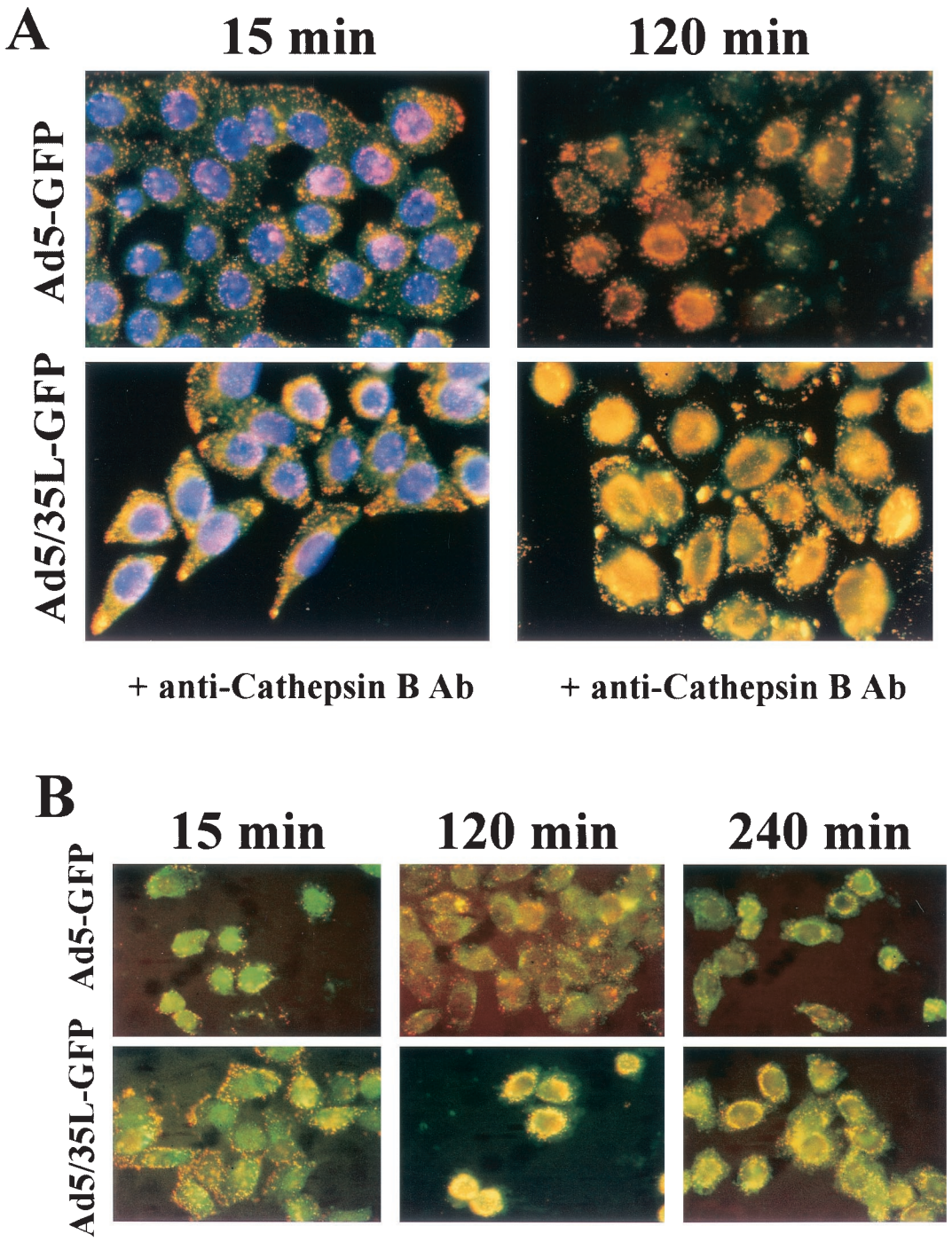

FIG. 3. Intracellular distribution of Ad vectors in HeLa cells. (A) Colocalization of Cy3-Ad particles (red) with Cathepsin B containing compartments (green) at 15 and 120 min postinitiation of virus infection. Note that Ad5-GFP virus particles do not colocalize with Cathepsin B-containing endosomes/lysosomes. (B) The effect of nocodazole on intracellular distribution of Cy3-labeled virus particles (red) and their colocalization with Cathepsin B-positive endosomes/lysosomes (green) in HeLa cells. Note rapid accumulation of Ad5/35L-GFP virus particles at the nucleus periphery and their strong colocalization with Cathepsin B-containing compartments. Ab, antibody.

formed transduction studies in the presence of agents that affect the endosomal/lysosomal pathway (Fig. 5). Enhancement of endosomal acidification by phorbol myristate acetate (PMA) (34) increased the transduction with Ad5 to a higher degree than transduction of Ad5/35L, indicating that acidification and early endosomal release of viral particles is an important step in Ad5 trafficking but not in trafficking of Ad5/35L. The lysosomal protease inhibitor, MG132 (8), significantly reduced the transduction of Ad5/35L but not that of Ad5. This suggests that passing through lysosomes and, possibly, processing of viral particles within lysosomes is involved in Ad5/35L trafficking.

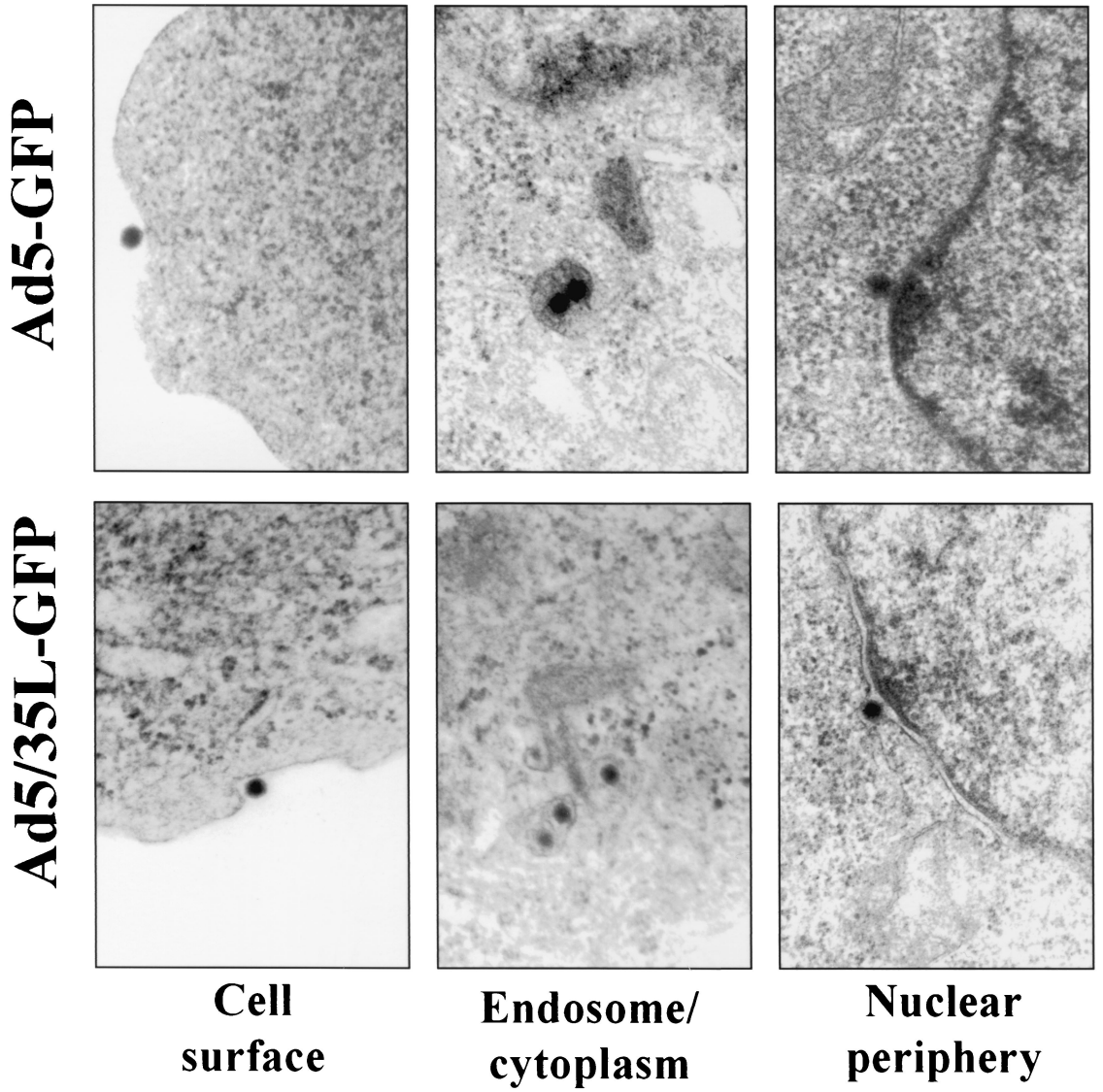

FIG. 4. Electron microscopic visualization of virus particles colocalized with different intracellular compartments. Magnification, ×35,000.

Taken together, these data demonstrate that although only the fiber knob domain was different between Ad5-GFP and Ad5/35L-GFP vectors, they selected different intracellular trafficking routes. Ad5-GFP virus efficiently escaped from the endosomal environment early after infection. By 2 h postinfection the majority of Ad5-GFP particles could be found free in the cytoplasm or accumulated at the perinuclear space. In contrast, Ad5/35L-GFP virus entered late endosomal/lysosomal compartments and remained there for at least 2 h. Some of the Ad5/35L-GFP virions reached the nucleus within late endosomes/lysosomes. Other virions appeared to be transported in a retrograde manner and deposited in or around adhesion foci at the cell surface.

The length of the fiber shaft does not affect the selection of intracellular trafficking routes by Ad vectors. Different trafficking pathways have been reported for wild-type Ad5 and Ad7 viruses as well as for Ad5 vector possessing Ad7 fibers (Ad5/7 capsid chimera). Studies by Miyazawa et al. demonstrated that chimeric Ad5/7 capsids accumulated in intracellular endosomal compartments, while Ad5 capsids remained dispersed in the cytoplasm (14). The authors concluded that specific structures within the Ad7 fiber act as a pH-dependent trigger allowing for endosomal membrane lysis and escape of the partially disassembled capsids to the cytosol. From their studies, however, it was not possible to conclude which fiber

TABLE 1. Intracellular distribution of Ad vectors in HeLa cells 2 h postinfection

Cellular compartment	% Distribution	
	Ad5-GFP	Ad5/35L-GFP
Endosome	3	62.6
Cytoplasm	52.4	13.3
Perinuclear space	35.1	19.3
Cell periphery	9.5	4.8

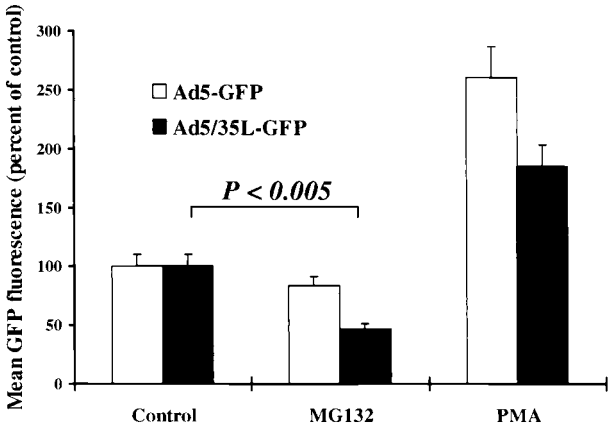

FIG. 5. Effect of MG132 and PMA on infectivity of Ad5-GFP and Ad5/35L-GFP vectors on HeLa cells. Cells (2×10^5 cells per well on a 12-well plate) were incubated with MG132 (40 μM) or PMA (100 nM) for 30 min before virus infection at 37°C. Then Ad5-GFP or Ad5/35L-GFP virus was added to the cells at an MOI of 400 virus particles per cell, and the cells were further incubated for 1 h. Virus-containing media were then removed and the percentage of GFP-expressing cells as well as the mean GFP fluorescence intensity were determined by flow cytometry 24 h postinfection. Under these infection conditions over 95% of cells expressed GFP. The transduction efficiency is expressed as the mean GFP fluorescence in the presence of MG132 or PMA compared to the mean fluorescence of cells infected in the absence of drug (Control). $n = 3$.

domain was responsible for the observed differences in intracellular trafficking between Ad5 and the Ad5/7 chimera, since in addition to different knob domains the Ad7 fiber also had a shortened shaft domain (7 pseudorepeats) compared to that of Ad5 (22 pseudorepeats). To investigate a potential role for the fiber shaft length in the process of selecting intracellular trafficking routes, we compared the pattern of intracellular virus distribution for Ad5-GFP and Ad5/35L-GFP to vectors with identical capsids and fiber knob domains but with short (S) fiber shaft domains, designated Ad5S and Ad5/35S (21). By using the techniques described above, HeLa cells were infected with Cy3-labeled Ad vectors and the pattern of Ad distribution within the cells was analyzed 15 min and 2 h postinfection (Fig. 6). Both vectors showed trafficking patterns similar to those depicted in Fig. 2 independent of the length of the fiber shaft domain. This demonstrates that the selection of intracellular trafficking routes is determined primarily by the fiber knob domain and by the nature of the primary attachment receptor and does not depend on the length of the fiber shaft.

Ad migration to late endosomal/lysosomal compartments decreases the efficiency of virus infection. To investigate whether the differential trafficking routes selected by Ad5-GFP and Ad5/35L-GFP vectors affect the efficiency of gene transfer, we analyzed reporter (GFP) gene expression after infection of HeLa cells with different MOIs of Ad5-GFP and Ad5/35L-GFP vectors. This analysis showed that the percentage of GFP-expressing cells after Ad5/35L-GFP infection was comparable or even lower than that after Ad5-GFP infection (Fig. 7A). Comparing the mean fluorescence intensity of GFP expression, the difference between the vectors was even more dramatic, especially at low MOIs. This observation was somewhat surprising, since three times more Ad5/35L-GFP particles initially attached to and internalized into cells than that of the Ad5-GFP vector (Fig. 1A, B). These data indicate that a large number of Ad5/35L-GFP genomes did not reach the nucleus. There are at least three potential explanations for this phenomenon.

(i) Ad5/35L-GFP genomes could be degraded within lysosomes. To investigate this possibility HeLa cells were infected with viral doses, which provided equivalent numbers of attached and internalized Ad5-GFP and Ad5/35L-GFP virus particles per cell. By using quantitative Southern blotting we analyzed the amounts of cell-associated Ad DNA at different time points postinfection (1, 8, and 24 h). Compared to the time point where virus particles were allowed to attach only to HeLa cells without internalization (0 h), we found no significant differences in the amounts of viral genomes for both viruses, suggesting that a complete intralysosomal degradation was not the primary pathway of Ad5/35L-GFP vector inactivation (data not shown).

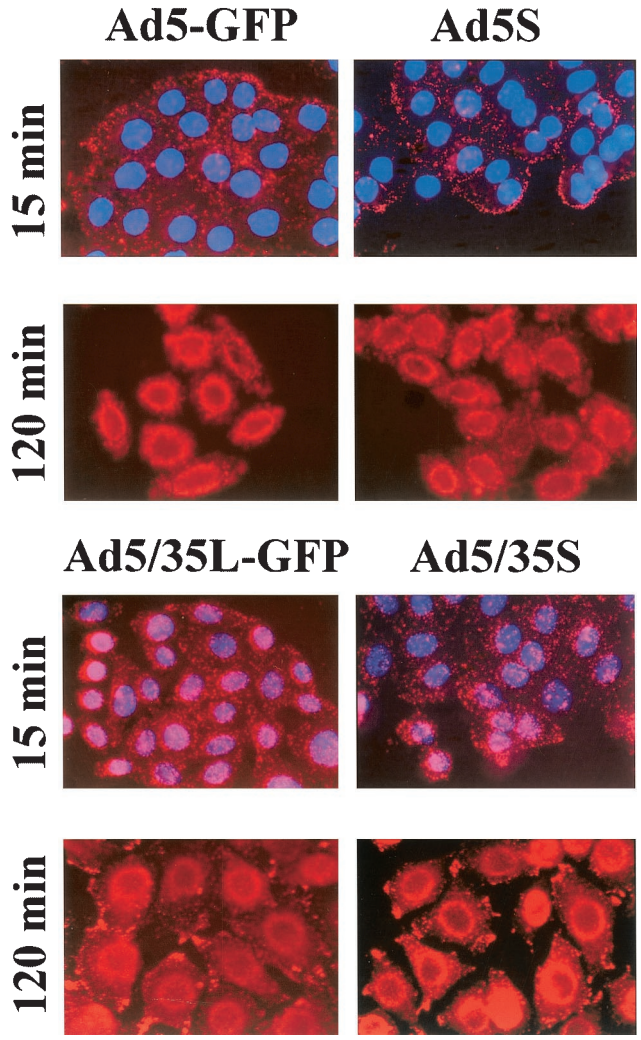

FIG. 6. The role of the fiber shaft domain length on the pattern of intracellular virus distribution at 15 min and 2 h postinitiation of virus infection. At 15 min postinfection cell nuclei were counterstained with 4′,6′-diamidino-2-phenylindole. Magnification, ×200.

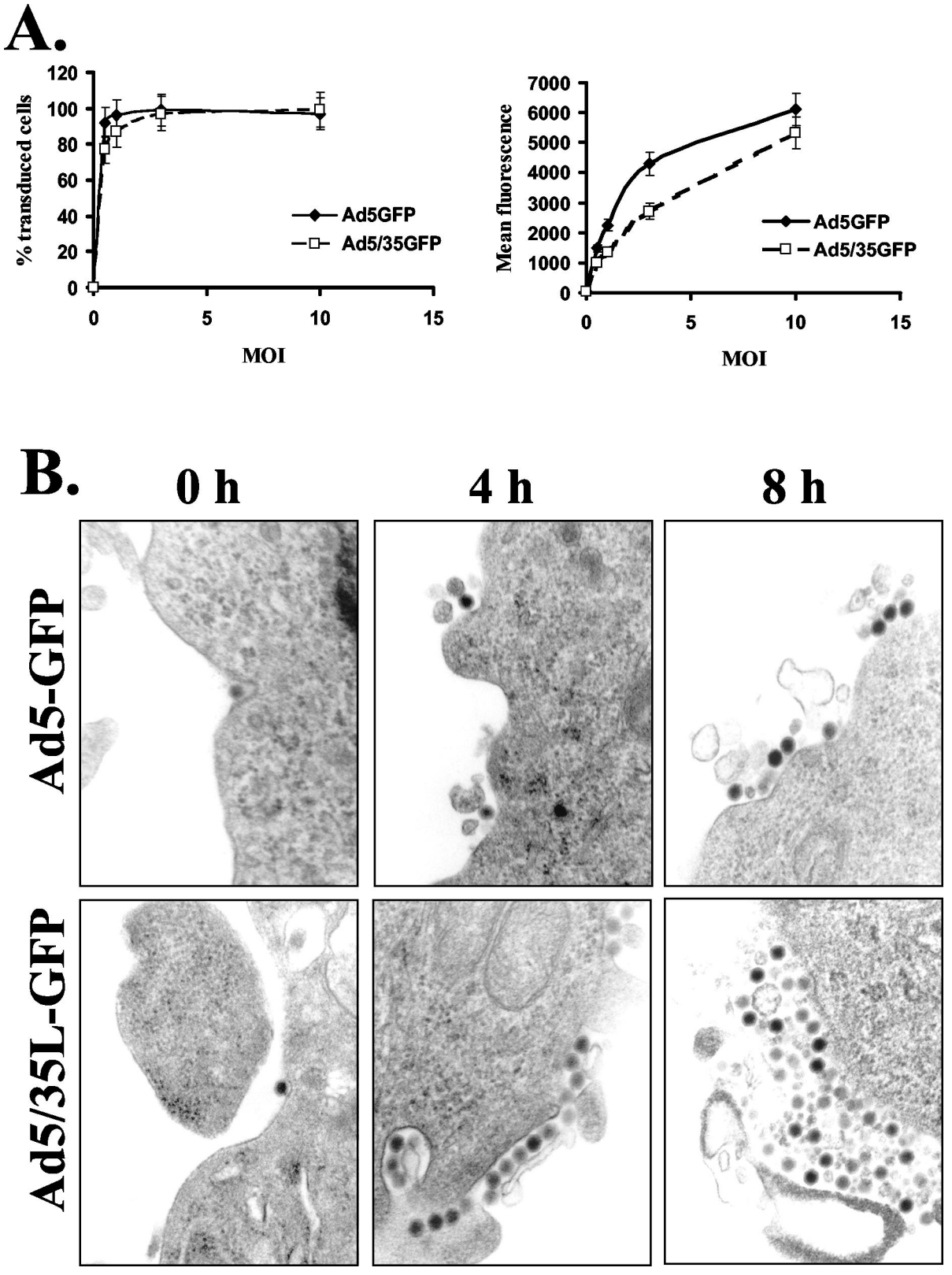

FIG. 7. (A) Infectivity of Ad5-GFP and Ad5/35L-GFP vectors on HeLa cells at different MOIs (PFU per cell). $n = 5$. (B) Electron microscopic visualization of virus particles on the HeLa cell surface at early (0 h) and late (4 and 8 h) time points postinfection. Magnification, ×35,000.

(ii) Viral particles residing for longer times within the endosomal compartments could be recycled back to the cell surface and released from the cell. To evaluate this possibility, we analyzed the virus distribution within infected HeLa cells at later time points after infection (4 and 8 h postinfection) by EM (Fig. 7B). In contrast to the time point of initiation of infection (0 h), when virions were found as single particles on the cell surface, at 4 and 8 h postinfection no single viral particles were visible outside the cells. Instead, relatively large conglomerates of viral particles associated with cellular debris were found for both Ad5-GFP- and Ad5/35L-GFP-infected cells. A quantitation of these virus-containing conglomerates located on the outer surface of cells revealed that more than 20% of HeLa cells infected with Ad5/35L-GFP had these virus depositions, while less than 3% of Ad5-GFP-infected cells accumulated virus particles on the cell surface at 4 and 8 h postinfection. Notably, the size of virus-containing conglomerates was larger for Ad5/35L-GFP-infected cells than for Ad5-GFP-infected counterparts. Considering the immunofluorescence data showing that Ad5/35L-GFP particles were deposited in areas near cell adhesion foci, these conglomerates apparently contain virus particles exported from the cell.

(iii) Interactions with disparate primary attachment receptors may differently affect the Ad disassembling program or suppress the ability of Ad5/35L-GFP virions to release the fiber and/or the escape from endosomes. For Ad5, it is known that the interaction with CAR and integrins results in fiber release and efficient escape from endosomes (16). To analyze whether the interaction with the Ad35 receptor can affect the infectivity of Ad5/35L virus particles, both Ad5 and Ad5/35L viruses were allowed to attach to HeLa cells on ice for 1 h at a dose that would yield an equal attachment level (Fig. 8). After nonattached virus particles were washed out, cells were freeze-thawed four times to release receptor-associated virus or were transferred to 37°C for 15 or 30 min. The Ad particles were then released by four freeze-thaw cycles, and dilutions of HeLa cell lysates were further applied on 293 cells for titering the Ad infectivity based on β-galactosidase transgene expression and the percentage of GFP-expressing cells. This analysis demonstrated that the binding of Ad5/35L particles to Ad35 receptors reduced their infectivity to a higher degree than that of Ad5 upon its binding to CAR. The differences between Ad5 and Ad5/35L became more apparent after a short incubation at 37°C.

Taken together, our data demonstrate that the interaction with a receptor different from CAR, although more efficient in attachment, results in a lower efficiency of gene transfer, probably by trapping the majority of virus particles in late endosomal/lysosomal cellular compartments or directing them away from the nucleus. This plus-end-directed transport is microtubule dependent and nocodazole sensitive. Furthermore, the binding of Ad5/35 particles to the Ad35 receptor leads to a more severe loss in virus infectivity compared to that of Ad5 binding to CAR.

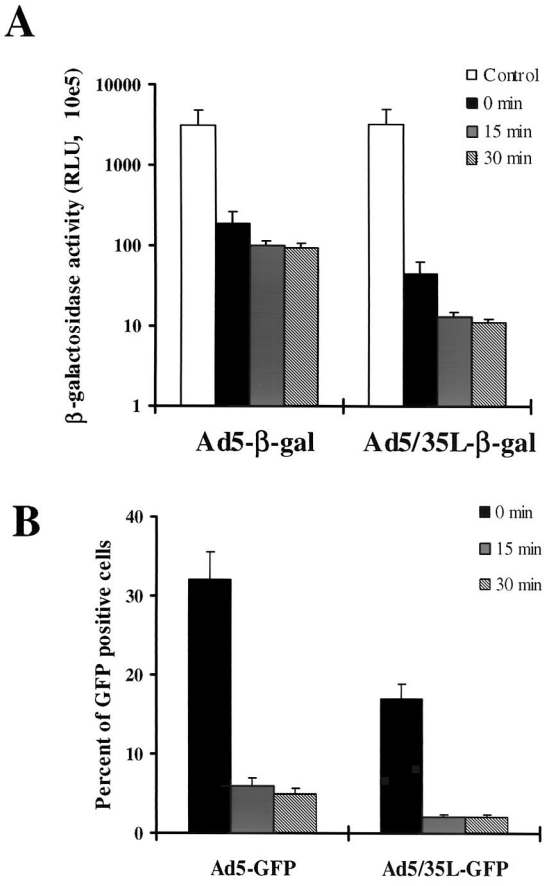

FIG. 8. Infectivity of Ad vectors on 293 cells after their recovery at different time points from infected HeLa cells by freeze-thawing. HeLa cells were infected on ice with Ad5 or Ad5/35L vectors expressing β-galactosidase (A) or GFP (B) under conditions that provide equivalent Ad attachment. Unattached virus particles were then removed and cells were transferred to 37°C for different times and were subjected to four freeze-thaw cycles to release cell-associated virus particles. In the control settings (0 min) cells with attached viruses were lysed without incubation at 37°C. HeLa cell lysates were obtained and applied on 293 cells, and the β-galactosidase activity or the percentage of GFP-expressing cells was analyzed 24 h later. All infections were performed in triplicate. The capsids of Ad5–β-gal and Ad5/35L–β-gal were identical to those of Ad5-GFP and Ad/35L-GFP, respectively. RLU, relative light units.

DISCUSSION

To evaluate our hypothesis that the primary attachment receptor largely determines the selection of intracellular trafficking routes by wild-type or capsid-modified Ads, we used Ad vectors with identical capsids except for the fiber knob domain, which is the capsid moiety responsible for high-affinity virus attachment to cell surface receptors. Intracellular trafficking was studied by using a number of methods, including chemically tagging Ad particles with a fluorophore, Cy3, direct detection by immunostaining of capsid hexon protein present in the incoming virus particles, and EM. All methods delivered comparable results, indicating that the chemical modification of Ad capsids does not affect structures involved in Ad trafficking. Our study demonstrates that Ad5 and Ad5/35 viruses select different intracellular trafficking routes upon interaction with different attachment receptors. The major difference in the trafficking of Ad5 and Ad5/35 was that Ad5/35 virus particles were readily found in late endosomes/lysosomes for up to 4 h after infection, whereas Ad5 virus escaped rapidly to the cytosol and never colocalized with late endosomal/lysosomal

markers. EM analyses showed that at 2 h after virus infection, the majority (more than 80%) of Ad5 virus particles could be found as free particles in the cytoplasm and in the perinuclear space and only 3% were found in the endosomes (Table 1). However, at the same time point, more than 60% of Ad5/35L virions were found within endosomes. This is in agreement with observations made for wild-type subgroup B and C viruses (5, 7, 18) as well as with studies performed with chimeric Ad5/7 vectors (13, 14). The latter studies have shown that specific structures within the Ad7 fiber act as a pH-dependent trigger for membrane lysis, allowing virus to escape into the cytosol. In the present study with vectors possessing identical knobs and fiber shaft domains of different lengths, we can exclude that the fiber shaft contains any enzymatic activities required for lysis of endosomal membranes. Instead, we postulate that the ability of the fiber knob to interact with different attachment receptors accounts for the different trafficking pathways observed for Ad5 and Ad5/35 vectors independently of the length of the fiber shaft domain. CAR appears to be required only to hold the virus particle in a suitable position in order to allow α_v integrins to interact with the penton base. This interaction has been found to initiate the signaling allowing for virus internalization and endosome release (25). For the unknown Ad35 receptor this signaling might be absent or different, resulting in a different trafficking route for the incoming virus. Notably, Ad5/35L-GFP and Ad5-GFP vectors have identical capsids except for the fiber knob domain. This implies that both of these vectors have the same net charge of the capsid. This is important, considering that the net charge of the capsid may affect the pathway and efficiency of Ad internalization (23).

Another important finding that distinguishes our study from the study published by Miyazawa et al. was that a more efficient attachment and internalization of Ad5/35L vector did not translate into a higher efficiency of gene transfer or level of transgene expression. Our data indicate that this is at least in part a result of trapping a portion of the Ad5/35 particles in late endosomal/lysosomal cellular compartments and retrograde transport and deposition of internalized Ad particles in adhesion foci at the cell surface. This plus-end-directed transport (toward the cell periphery) was nocodazole sensitive. Only the part of Ad5/35L virus particles that reached the perinuclear space within late endosomes/lysosomes contributed to GFP expression. In general, molecules that enter cells via receptor-mediated endocytosis can follow one of two major routes: (i) the endocytic recycling pathway, in which membrane proteins and membrane-bound proteins are collected in a tubulovesicular compartment, termed the endocytic recycling compartment, prior to trafficking back to the cell surface; or (ii) the lysosomal pathway, in which a select set of membrane proteins, ligands that have dissociated from their receptors, and soluble materials occupy a compartment termed the sorting endosome, which later matures and acidifies to become a late endosome and finally a lysosome (15). In our case it appears that trafficking of Ad5/35L particles involves both pathways. Our data suggest that Ad5/35 particles achieve proximity to the nucleus by remaining inside late endosomes/lysosomes. Furthermore, from our data it appears that some of the Ad5/35 particles enter the endocytic recycling pathway and are released from the cell. Finally, in comparison to the Ad5-CAR interaction, the binding of Ad5/35 particles to the receptor may lead to more destructive changes in structures that determine the infectivity of Ad particles.

Other factors that may influence Ad5/35 trafficking remain to be investigated, including whether fiber release occurs during internalization and which signaling pathways are activated. The development of Ad vectors that interact with receptors different from CAR requires a better understanding of events that follow the internalization of viral particles. This study forms a basis for addressing potential problems associated with development and use of novel capsid-modified Ad vectors for gene therapy applications.

ACKNOWLEDGMENTS

Dmitry M. Shayakhmetov and Zong-Yi Li contributed equally to this work.

We thank Kathrin Bernt and Daniel Stone for critical discussion of the manuscript.

This work was supported by funding from NIH grants POI HL 53750 and HL-00-008 and a grant from the Cystic Fibrosis Foundation.

REFERENCES

1. **Bai, M., B. Harfe, and P. Freimuth.** 1993. Mutations that alter an Arg-Gly-Asp (RGD) sequence in the adenovirus type 2 penton base protein abolish its cell-rounding activity and delay virus reproduction in flat cells. J. Virol. **67:**5198–5205.
2. **Bergelson, J. M., J. A. Cunningham, G. Droguett, E. A. Kurt-Jones, A. Krithivas, J. S. Hong, M. S. Horwitz, R. L. Crowell, and R. W. Finberg.** 1997. Isolation of a common receptor for Coxsackie B viruses and adenoviruses 2 and 5. Science **275:**1320–1323.
3. **Blumenthal, R., P. Seth, M. C. Willingham, and I. Pastan.** 1986. pH-dependent lysis of liposomes by adenovirus. Biochemistry **25:**2231–2237.
4. **Carlson, C. A., D. S. Steinwaerder, H. Stecher, D. M. Shayakhmetov, and A. Lieber.** 2002. Rearrangements in adenoviral genomes mediated by inverted repeats. Methods Enzymol. **346:**277–292.
5. **Chardonnet, Y., and S. Dales.** 1970. Early events in the interaction of adenoviruses with HeLa cells. Virology **40:**462–485.
6. **Coonrod, A., F. Q. Li, and M. Horwitz.** 1997. On the mechanism of DNA transfection: efficient gene transfer without viruses. Gene Ther. **4:**1313–1321.
7. **Defer, C., M. T. Belin, M. L. Caillet-Boudin, and P. Boulanger.** 1990. Human adenovirus-host cell interactions: comparative study with members of subgroups B and C. J. Virol. **64:**3661–3673.
8. **Douar, A. M., K. Poulard, D. Stockholm, and O. Danos.** 2001. Intracellular trafficking of adeno-associated virus vectors: routing to the late endosomal compartment and proteasome degradation. J. Virol. **75:**1824–1833.
9. **Greber, U. F., M. Suomalainen, R. P. Stidwill, K. Boucke, M. W. Ebersold, and A. Helenius.** 1997. The role of the nuclear pore complex in adenovirus DNA entry. EMBO J. **16:**5998–6007.
10. **Greber, U. F., P. Webster, J. Weber, and A. Helenius.** 1996. The role of the adenovirus protease on virus entry into cells. EMBO J. **15:**1766–1777.
11. **Leopold, P. L., B. Ferris, I. Grinberg, S. Worgall, N. R. Hackett, and R. G. Crystal.** 1998. Fluorescent virions: dynamic tracking of the pathway of adenoviral gene transfer vectors in living cells. Hum. Gene Ther. **9:**367–378.
12. **Leopold, P. L., G. Kreitzer, N. Miyazawa, S. Rempel, K. K. Pfister, E. Rodriguez-Boulan, and R. G. Crystal.** 2000. Dynein- and microtubule-mediated translocation of adenovirus serotype 5 occurs after endosomal lysis. Hum. Gene Ther. **11:**151–165.
13. **Miyazawa, N., R. G. Crystal, and P. L. Leopold.** 2001. Adenovirus serotype 7 retention in a late endosomal compartment prior to cytosol escape is modulated by fiber protein. J. Virol. **75:**1387–1400.
14. **Miyazawa, N., P. L. Leopold, N. R. Hackett, B. Ferris, S. Worgall, E. Falck-Pedersen, and R. G. Crystal.** 1999. Fiber swap between adenovirus subgroups B and C alters intracellular trafficking of adenovirus gene transfer vectors. J. Virol. **73:**6056–6065.
15. **Mukherjee, S., R. N. Ghosh, and F. R. Maxfield.** 1997. Endocytosis. Physiol. Rev. **77:**759–803.
16. **Nakano, M. Y., K. Boucke, M. Suomalainen, R. P. Stidwill, and U. F. Greber.** 2000. The first step of adenovirus type 2 disassembly occurs at the cell surface, independently of endocytosis and escape to the cytosol. J. Virol. **74:**7085–7095.
17. **Ng, T., D. Shima, A. Squire, P. I. Bastiaens, S. Gschmeissner, M. J. Humphries, and P. J. Parker.** 1999. PKCα regulates β1 integrin-dependent cell motility through association and control of integrin traffic. EMBO J. **18:**3909–3923.
18. **Ogier, G., Y. Chardonnet, and W. Doerfler.** 1977. The fate of type 7 adenovirions in lysosomes of HeLa cells. Virology **77:**66–77.

19. **Reddy, P. S., S. Ganesh, P. M. Limbach, T. Brann, A. M. Pinkstaff, M. Kaleko, and S. Conelly.** 2002. Development of adenovirus serotype 35 as a gene transfer vector. Mol. Ther. **5:**S67.
20. **Shayakhmetov, D. M., Z. Y. Li, S. Ni, and A. Lieber.** 2002. Targeting of adenovirus vectors to tumor cells does not enable efficient transduction of breast cancer metastases. Cancer Res. **62:**1063–1068.
21. **Shayakhmetov, D. M., and A. Lieber.** 2000. Dependence of adenovirus infectivity on length of the fiber shaft domain. J. Virol. **74:**10274–10286.
22. **Shayakhmetov, D. M., T. Papayannopoulou, G. Stamatoyannopoulos, and A. Lieber.** 2000. Efficient gene transfer into human CD34(+) cells by a retargeted adenovirus vector. J. Virol. **74:**2567–2583.
23. **Soudais, C., S. Boutin, S. S. Hong, M. Chillon, O. Danos, J. M. Bergelson, P. Boulanger, and E. J. Kremer.** 2000. Canine adenovirus type 2 attachment and internalization: coxsackievirus-adenovirus receptor, alternative receptors, and an RGD-independent pathway. J. Virol. **74:**10639–10649.
24. **Stevenson, S. C., M. Rollence, J. Marshall-Neff, and A. McClelland.** 1997. Selective targeting of human cells by a chimeric adenovirus vector containing a modified fiber protein. J. Virol. **71:**4782–4790.
25. **Suomalainen, M., M. Y. Nakano, K. Boucke, S. Keller, and U. F. Greber.** 2001. Adenovirus-activated PKA and p38/MAPK pathways boost microtubule- mediated nuclear targeting of virus. EMBO J. **20:**1310–1319.
26. **Suomalainen, M., M. Y. Nakano, S. Keller, K. Boucke, R. P. Stidwill, and U. F. Greber.** 1999. Microtubule-dependent plus- and minus-end-directed motilities are competing processes for nuclear targeting of adenovirus. J. Cell Biol. **144:**657–672.
27. **Ternovoi, V., D. Stone, V. Sandig, and A. Lieber.** 2002. Adenovirus type 11 complements type 5 viral DNA replication but not packaging. Mol. Ther. **5:**S55.
28. **Tomko, R. P., R. Xu, and L. Philipson.** 1997. HCAR and MCAR: the human and mouse cellular receptors for subgroup C adenoviruses and group B coxsackieviruses. Proc. Natl. Acad. Sci. USA **94:**3352–3356.
29. **Wang, K., T. Guan, D. A. Cheresh, and G. R. Nemerow.** 2000. Regulation of adenovirus membrane penetration by the cytoplasmic tail of integrin β5. J. Virol. **74:**2731–2739.
30. **Wang, K., S. Huang, A. Kapoor-Munshi, and G. Nemerow.** 1998. Adenovirus internalization and infection require dynamin. J. Virol. **72:**3455–3458.
31. **Wang, X., and J. M. Bergelson.** 1999. Coxsackievirus and adenovirus receptor cytoplasmic and transmembrane domains are not essential for coxsackievirus and adenovirus infection. J. Virol. **73:**2559–2562.
32. **Wickham, T. J., P. Mathias, D. A. Cheresh, and G. R. Nemerow.** 1993. Integrins alpha v beta 3 and alpha v beta 5 promote adenovirus internalization but not virus attachment. Cell **73:**309–319.
33. **Zabner, J., M. Chillon, T. Grunst, T. O. Moninger, B. L. Davidson, R. Gregory, and D. Armentano.** 1999. A chimeric type 2 adenovirus vector with a type 17 fiber enhances gene transfer to human airway epithelia. J. Virol. **73:**8689–8695.
34. **Zen, K., J. Biwersi, N. Periasamy, and A. S. Verkman.** 1992. Second messengers regulate endosomal acidification in Swiss 3T3 fibroblasts. J. Cell Biol. **119:**99–110.
35. **Zinn, K. R., J. T. Douglas, C. A. Smyth, H. G. Liu, Q. Wu, V. N. Krasnykh, J. D. Mountz, D. T. Curiel, and J. M. Mountz.** 1998. Imaging and tissue biodistribution of 99mTc-labeled adenovirus knob (serotype 5). Gene Ther. **5:**798–808.